agronomy

MDPI

Article

TMT-Based Quantitative Proteomic Analysis Reveals the Response of Tomato (*Solanum lycopersicum* L.) Seedlings to Ebb-and-Flow Subirrigation

Kelei Wang [1,2], Muhammad Moaaz Ali [1,3], Tianxin Guo [1], Shiwen Su [2,4], Xianzhi Chen [2,4], Jian Xu [2,4,*] and Faxing Chen [1,*]

[1] College of Horticulture, Fujian Agriculture and Forestry University, Fuzhou 350002, China
[2] Wenzhou Vocational College of Science and Technology, Wenzhou 325014, China
[3] College of Plant Protection, Fujian Agriculture and Forestry University, Fuzhou 350002, China
[4] Wenzhou Protected Vegetable Engineering Technology Center, Wenzhou 325014, China
* Correspondence: xujian@wzvcst.edu.cn (J.X.); cfaxing@126.com (F.C.)

Abstract: Ebb-and-flow subirrigation (EFI) is a water-saving and environmentally friendly irrigation method that can effectively improve water use efficiency and promote plant growth. In this study, we elucidated the effects of ebb-and-flow subirrigation on the protein levels in tomato roots in comparison with top sprinkle irrigation (TSI) and used an integrated approach involving tandem mass tag (TMT) labeling, high-performance liquid chromatography (HPLC) fractionation, and mass-spectrometry (MS)-based analysis. A total of 8510 quantifiable proteins and 513 differentially accumulated proteins (DAPs) were identified, of which the expressions of 283 DAPs were up-regulated, and 230 DAPs were down-regulated in the EFI vs. TSI treatment comparison. According to proteomic data, we performed a systematic bioinformatics analysis of all the identified proteins and DAPs. The DAPs were most significantly associated with the terms 'metabolic process', 'anchored component of membrane', 'oxidoreductase activity', 'phenylpropanoid biosynthesis', and 'biosynthesis of secondary metabolites' according to Gene Ontology (GO) and Kyoto Encyclopedia of Genes and Genomes enrichment (KEGG) analysis. The 272 DAPs were classified into 12 subcellular components according to their subcellular localization. Furthermore, the activities of SOD, POD, CAT, GR, and APX in tomato roots were remarkably increased under EFI, while the MDA content was decreased compared with TSI. Correlation analysis among activities of enzymes and their related DAPs showed that 30 DAPs might be responsible for the regulation of these enzymes. The results showed that ebb-and-flow subirrigation could induce a series of DAPs responses in tomato roots to be adapted to the new mode of water supply.

Keywords: irrigation; root-softening; antioxidant; ebb-and-flow; tandem mass tag; HPLC-MS

Citation: Wang, K.; Ali, M.M.; Guo, T.; Su, S.; Chen, X.; Xu, J.; Chen, F. TMT-Based Quantitative Proteomic Analysis Reveals the Response of Tomato (*Solanum lycopersicum* L.) Seedlings to Ebb-and-Flow Subirrigation. *Agronomy* **2022**, *12*, 1880. https://doi.org/10.3390/agronomy12081880

Academic Editors: Roxana Yockteng, Andrés J. Cortés and María Ángeles Castillejo

Received: 7 July 2022
Accepted: 7 August 2022
Published: 10 August 2022

1. Introduction

Tomato (*Solanum lycopersicum* L.) belongs to the Solanaceae family and is a greenhouse vegetable crop native to Peruvian and Mexican regions [1,2]. It is a rich source of natural antioxidants, including flavonoids; carotenoids (mainly lycopene and β-carotene); and vitamins A, B, and C [3–7]. Vegetable production in the greenhouse demands high fertilizer and water inputs in order to achieve better yield and superior-quality produce [8–11]. The top sprinkle irrigation system (TSI) is a common irrigation strategy for greenhouse vegetable production that is not regarded as ecologically friendly since significant amounts of water and nutrients are usually wasted and may runoff/leach, damaging surface and groundwater systems [12–14]. Besides, the seedlings around the hole plate grow poorly due to water shortage, resulting in inconsistent seedling height [15–17].

An evolved form of the continuous floating system, the ebb-and-flow irrigation (EFI) system was originally developed to grow tobacco (*Nicotiana tabacum* L.) plants in order to

increase field survival and reduce transplant shock. It is now being used to grow a large number of commercial vegetables in China, Japan, the United States, and other developing countries [18]. It has many advantages, such as root moisture optimization, water saving, and fertilizer saving compared to top sprinkler irrigation [19–21]. Metal wires ≈ 0.20 m are used to suspend the seedling trays above the concrete floor. Every two to three days, the irrigation water is brought up to the level of the trays, held there for 15 to 45 min, and then returned to the main reservoir until the next irrigation. In this system, water or nutrient solution is transported to the plant root through the bottom of the cultivation container by capillary action of the cultivation medium, which can effectively avoid the edge or umbrella effect and improve plant uniformity [18,22,23]. A number of studies in subirrigation, which have been primarily carried out with ornamental species, have demonstrated that the concentration of the nutrient solution can be reduced by up to 50% when compared to nutrient solutions for top sprinkle irrigation, with no adverse effects on plant growth or quality [10,24]. Subirrigation systems improved the uniformity and quality of bell pepper (*Capsicum annum* L.) and tomato (*S. lycopersicum* L.) if grown with minimal nutrient and drought stress [25–27].

Different irrigation methods cause differences in root growth [28]. However, waterlogging and anaerobic respiration over an extended period of time result in the buildup of aldehydes, as well as an increase in reactive oxygen species (ROS), which finally leads to cell death and plant senescence [29,30]. Plant hormones may accumulate or degrade quickly if the gaseous exchange is hampered, and this can alter plant waterlogging tolerance [31,32]. When plants are under waterlogging or drought stress, the activities of protective enzymes in plants change dynamically [33,34]. In a recent study, the activities of superoxide dismutase (SOD), peroxidase (POD), catalase (CAT), and other protective enzymes in the roots of sesame seedlings increased at the initial stage of flooding and decreased significantly with the extension of the water stress time [35,36].

A novel tandem-mass-spectrometry (MS)-based tandem mass tag (TMT) labeling strategy has been used in quantitative proteomics in recent years [37–39]. Therefore, we used a TMT-based quantitative proteomics approach to identify differentially accumulated proteins (DAPs) in tomato roots under ebb-and-flow subirrigation so as to provide a theoretical basis for the popularization and application of ebb-and-flow irrigation technology.

2. Materials and Methods

2.1. Plant Source, Experimental Design, and Irrigation Treatments

The experiment was conducted at the experimental farm of Wenzhou Vocational College of Science and Technology, Wenzhou, China (28°05′39.5″ N 120°30′55.2″ E) from 15 August 2019 to 19 September 2019. The pure line tomato cultivar 'Ouxiu 201' (round-shaped fruit with regular leaves) was obtained from Institute of Vegetable Science, Wenzhou Academy of Agricultural Sciences, Wenzhou, China. Tomato seeds were sown in seedlings trays (540 mm × 280 mm) with 50 plugs (each having volume of 55 mL with upper and lower diameters of 48 and 18 mm, respectively). Seedling trays were purchased from Taizhou Longji Plastics Co., Ltd., Taizhou, China. Seedling plugs were filled with growing media containing peat, vermiculite, and perlite (3:1:1), which were obtained from Hangzhou Lin'an Jindalu Industrial Technology Co., Ltd., Hangzhou, China. The pH, EC, and organic matter of the growing media were 6.34, 0.87 ms·cm^{-1}, and 95.4%, respectively. The ebb-and-flow irrigation system (patent no. *ZL201520333950*.6) used in the experiment was developed by Wenzhou Academy of Agricultural Sciences, Wenzhou, China. It contained a nursery frame, a number of ebb-and-flow trays horizontally placed on the nursery frame, and a water or nutrient solution circulation device (Figure 1).

Tomato seedling trays were placed on ebb-and-flow irrigation (EFI) seedling raising system [40], as well as on simple beds for top sprinkle irrigation (TSI) water treatment. The top sprinkle irrigation was carried out by manually holding the watering can. There was no fertilizer applied during the experiment. Six seedling trays were used for this experiment, each being considered as a replication of different irrigation treatments, i.e., EFI and TSI.

Each irrigation treatment had 3 repetitions with 50 plants in each repeat. The experiment was a completely randomized design (CRD).

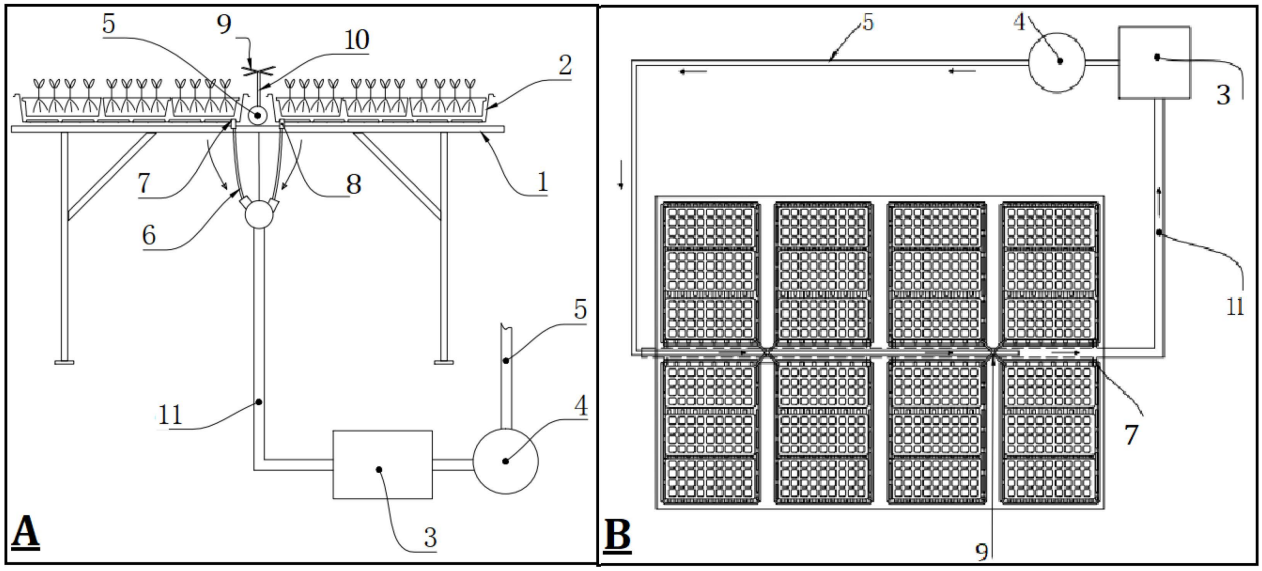

Figure 1. Lateral (**A**) and top (**B**) view of ebb-and-flow nursery raising system. 1—nursery frame; 2—ebb-and-flow tray; 3—water reservoir; 4—disinfection equipment; 5—inlet main pipe; 6—drainage branch pipe; 7—drainage hole; 8—filtering parts; 9—inlet branch pipe; 10—five-way connector; 11—drainage main pipe.

2.2. Enzymes' Activity Assay

Thirty-five days after sowing, root samples (0.5 g) were collected from ten randomly selected seedlings from each replication of each irrigation treatment and quickly frozen in liquid nitrogen. Then, 1 mL of 0.1 M phosphoric acid buffer (pH = 7) was added into frozen root samples, ground, and homogenized in an ice bath. The final volume of 5 mL was made by adding 0.1 M phosphoric acid buffer (pH = 7), and 2 mL was taken and centrifuged at 10,000 rpm for 10 min. The supernatant was obtained as the crude extract of enzyme solution [41] and stored at 4 °C for further analysis.

The activity of superoxidase dismutase (SOD; EC 1.15.1.1) was assayed using a xanthine–xanthine oxidase system [42]. The change in absorbance was read at 560 nm. Peroxidase (POD; EC 1.11.1.7) activity was determined using a previously described method [43]. The change in absorbance was read at 470 nm for 4 min. Catalase (CAT; EC 1.11.1.6) activity was assayed as described previously [44]. The reaction was initiated with the enzyme extract. The decrease in absorbance (due to decomposition of H_2O_2) at 240 nm was recorded for 1 min. Ascorbate peroxidase (APX; EC 1.11.1.11) activity was measured as previously described by Nakano and Asada [45]. The absorbance was measured at 290 nm for 1 min. The activity of glutathione reductase (GR; EC 1.6.4.2) was measured using the method earlier described by Cakmak et al. [46]. The decrease in absorbance was recorded for 1 min at 340 nm due to NADPH oxidation.

2.3. Protein Extraction, TMT Labeling, and Data Analysis

Total proteins were extracted from the EFI and TSI root tissues of tomato with three biological replicates (each containing 500 mg roots) using the cold acetone method [47]. Next, the tryptic peptides of each sample were labeled through tandem mass tags (TMT) using a TMT kit (Novogene Bio Technology Co., Ltd., Nanjing, China) according to the manufacturer's protocol, and TSI1, TSI2, TSI3, EFI1, EFI2, and EFI3 were labeled with 126, 127 N, 128 N, 129 N, 130 N, and 131 tags, respectively. Then, they were fractionated by high-pH reverse-phase HPLC using a C18 column (Waters BEH C18 4.6 × 250 mm, 5 µm) on a Rigol L3000 HPLC system. These peptides were further used for proteomic analysis. Proteome

analysis for the fractionated peptides was performed using a liquid chromatography–mass spectrometry (LC-MS) system. Briefly, these peptides were performed using an EASY-nLCTM 1200 UHPLC system (Thermo Fisher Scientific Co., Ltd., Shanghai, China) coupled with a Q Exactive HF-X mass spectrometer (Thermo Fisher Scientific Co., Ltd., Shanghai, China) operating in the data-dependent acquisition (DDA) mode. A total of 1 µg sample was injected into a home-made C18 Nano-Trap column (2 cm × 75 µm, 3 µm). Peptides were separated in a home-made analytical column (15 cm × 150 µm, 1.9 µm) using a linear gradient elution. The separated peptides were analyzed by Q Exactive HF-X mass spectrometer (Thermo Fisher Scientific Co., Ltd., Shanghai, China), with ion source of Nanospray Flex™, spray voltage of 2.3 kV, and ion transport capillary temperature of 320 °C. Full scan range from 350 to 1500 m/z with resolution of 60,000 (at 200 m/z), automatic gain control (AGC) target value of 3×10^6, and a maximum ion injection time of 20 ms were used. The top 40 precursors of the highest abundant in the full scan were selected and fragmented by higher-energy collisional dissociation (HCD) and analyzed in MS, where resolution was 30,000 (at 200 m/z) for 6 plex, the automatic gain control (AGC) target value was 5×10^4, the maximum ion injection time was 54 ms, the normalized collision energy was set as 32%, the intensity threshold was 1.2×10^5, and the dynamic exclusion parameter was 20 s.

The resulting spectra from each run were searched separately against protein sequences library (Solanum_lycopersicum.SL3.0.pep.all.fasta, 34,429 sequences) database by the search engines: Proteome Discoverer 2.2 (PD 2.2, Thermo). The searched parameters were set as follows: mass tolerance for precursor ion was 10 ppm, and mass tolerance for product ion was 0.02 Da. Carbamidomethyl was specified as fixed modifications, oxidation of methionine (M) and TMT plex were specified as dynamic modification, and acetylation and TMT plex were specified as N-Terminal modification in PD 2.2. A maximum of 2 mis-cleavage sites were allowed. The principal component analysis (PCA) was used to evaluate the relationship among 6 samples. T-test was used to compare the differentially accumulated proteins (DAPs). Proteins with fold change (FC) > 1.5 or <0.67 and $p \leq 0.05$ were considered as DAPs. Notably, the protein quantification was calculated with the median ratio of its corresponding unique peptides and then normalized by taking the median of all quantified proteins.

2.4. Data Analysis

Data regarding antioxidant enzymes were subjected to Student's t-test using Microsoft Excel (ver. 2016). Correlation between antioxidant enzymes' activities and their metabolism-related proteins was determined with Pearson (n) method using IBM SPSS software (ver. 17.0) and visualized through a heatmap using TBtools software (ver. 0.6655) [48]. Principal components analysis (PCA) was performed using SIMCA-P (version 11.5) software. Gene Ontology (GO) functional analysis was conducted using the InterProScan program against the non-redundant protein database (including Pfam, PRINTS, ProDom, SMART, ProSite, PANTHER) [49], and the databases of COG (Clusters of Orthologous Groups) and KEGG (Kyoto Encyclopedia of Genes and Genomes) were used to analyze the protein families and pathways. DAPs were used for volcanic map analysis and enrichment analysis of GO and KEGG [50]. Subcellular localizations of DAPs were predicted using WoLF PSORT (https://wolfpsort.hgc.jp/ (accessed on 14 January 2022), Loctree 3 (https://rostlab.org/services/loctree3/ (accessed on 14 January 2022), TargetP (http://www.cbs.dtu.dk/services/TargetP/ (accessed on 16 January 2022), and SignalP (http://www.cbs.dtu.dk/services/SignalP/ (accessed on 16 January 2022) [51–54].

3. Results

3.1. Primary Quantitative Proteome Analysis

Based on the TMT experiment, a total of 337,532 spectra were identified from tomato roots. Moreover, 61,531 peptides, 50,462 unique peptides, and 8510 proteins were detected from 93,451 known spectra (Figure 2A). The protein molecular weight data (Figure 2B) showed that 82.28% of the total proteins were 10–80 kDa in size, and the average molecular

weight was 8.25–274.25 kDa. In addition, about 91% of proteins' sequence coverage was less than 40% (Figure 2C). The length of most peptides was between 7 and 25 amino acids (aa) (Figure 2D), accounting for 97.29% of the total, of which peptides with a length of 8–12 aa were relatively large.

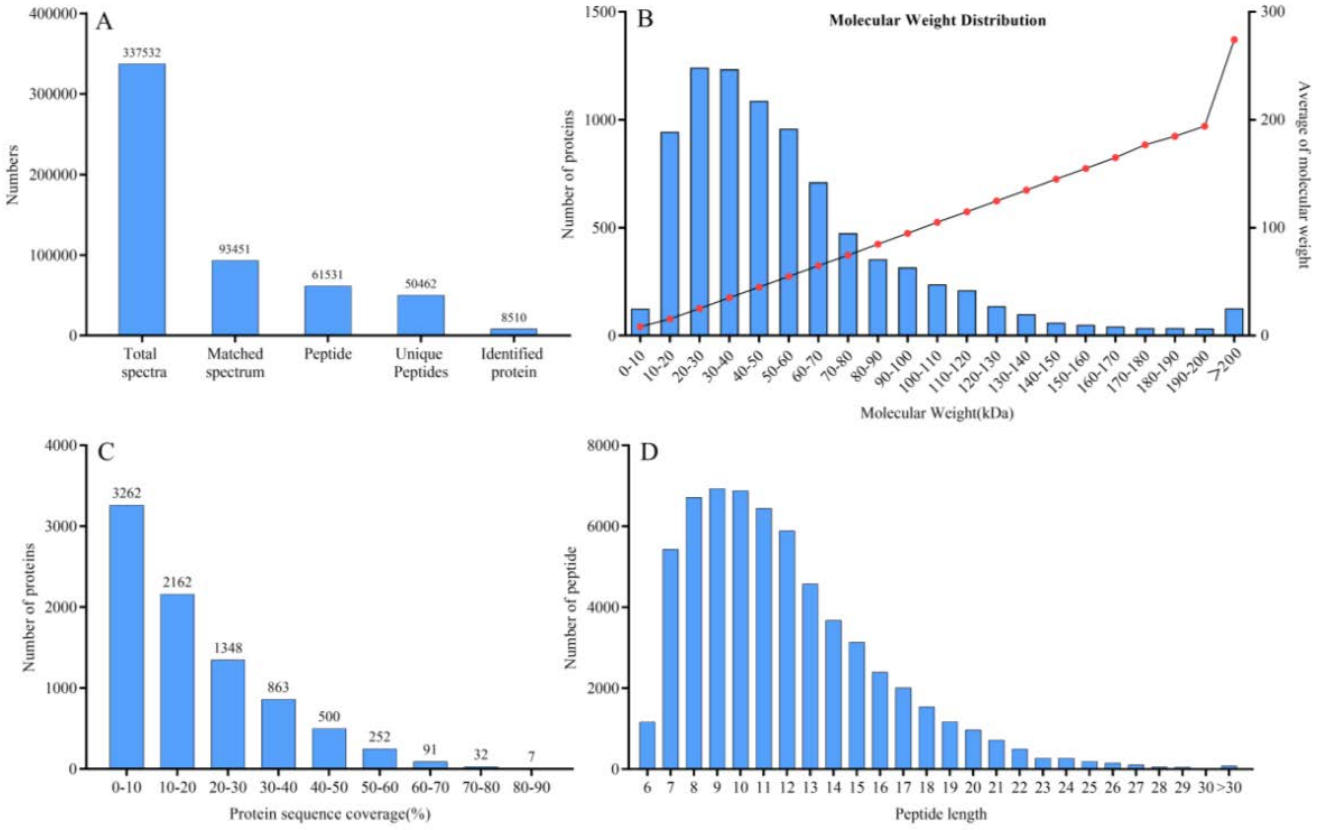

Figure 2. Quality control (QC) validation of mass spectrometer (MS) data. (**A**) Basic statistical data of MS results. (**B**) Molecular weight distribution of proteins. (**C**) Proteins' sequence coverage. (**D**) Length distribution of all identified phosphorylated peptides.

To assess the reproducibility of proteomic data, the coefficient of variation of replicates was determined. Proteins having a 20 percent coefficient of variation accounted for more than 90% of detected proteins (Figure 3A), indicating that the data were credible. EFI and TFI data were cleanly differentiated in a PCA model based on six samples (Figure 3B). PCA1 was responsible for 75.26 percent of the variability, whereas PCA2 was responsible for 13.98 percent.

3.2. Effect of EFI Treatment on the Global Proteome of Tomato Seedlings

The identified proteins and DAPs of tomato roots under ebb-and-flow subirrigation were grouped into three GO categories (biological process, cellular component, and molecular functions) (Figure 4A, Table S1). We can see that in the biological process (BP), 586 identified proteins (including 160 DAPs) were involved in the oxidation-reduction process, 357 proteins (12 DAPs) were involved in protein phosphorylation, and 288 proteins (25 DAPs) were involved in metabolic process. In the cellular component, 278 identified proteins (including 9 DAPs) were involved in integral components of the membrane, 251 proteins (18 DAPs) were involved in membrane synthesis, and 169 proteins (2 DAPs) were involved in the nucleus. In the molecular functions category, 903 identified proteins (including 30 DAPs) were involved in protein binding, 765 proteins (30 DAPs) were involved in ATP binding, whereas 356 identified proteins (12 DAPs) were involved in protein kinase activity.

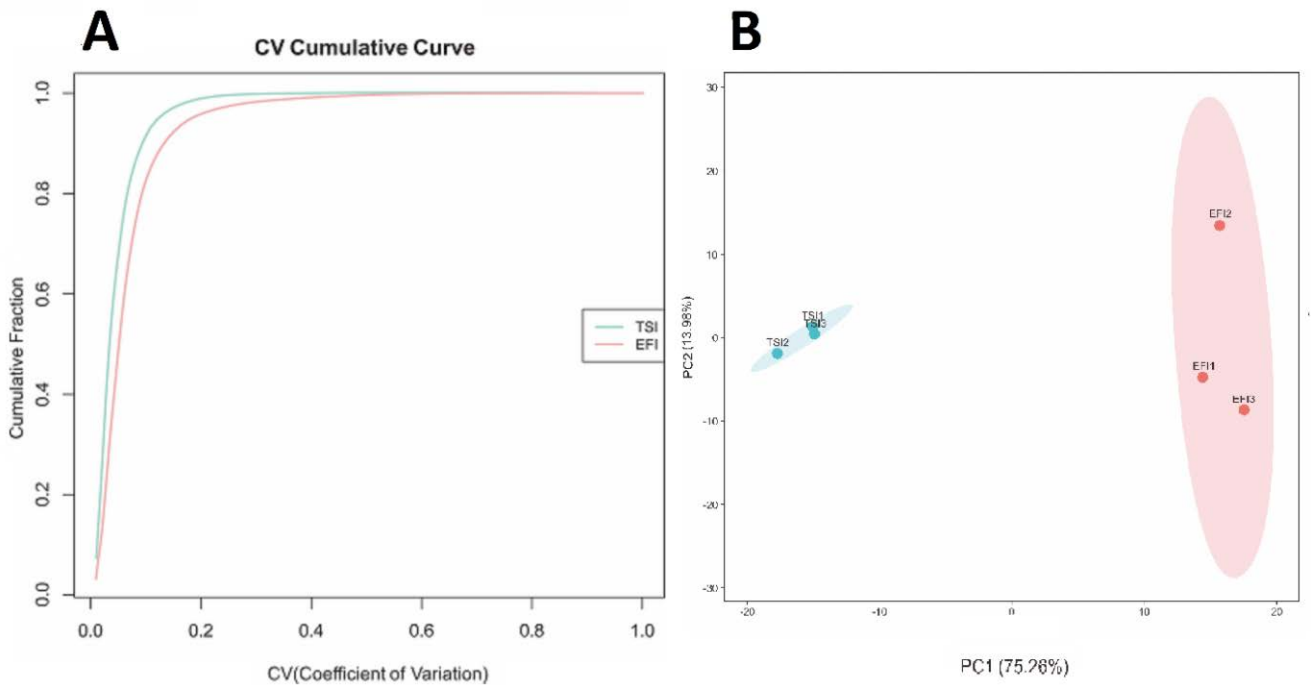

Figure 3. Scatter plot of CV (coefficient of variation) distribution and PCA (principal component analysis) of all samples using quantified proteins. (**A**) CV cumulative curve of two treatments. (**B**) Two-dimensional scatter plot of PCA distribution of all samples.

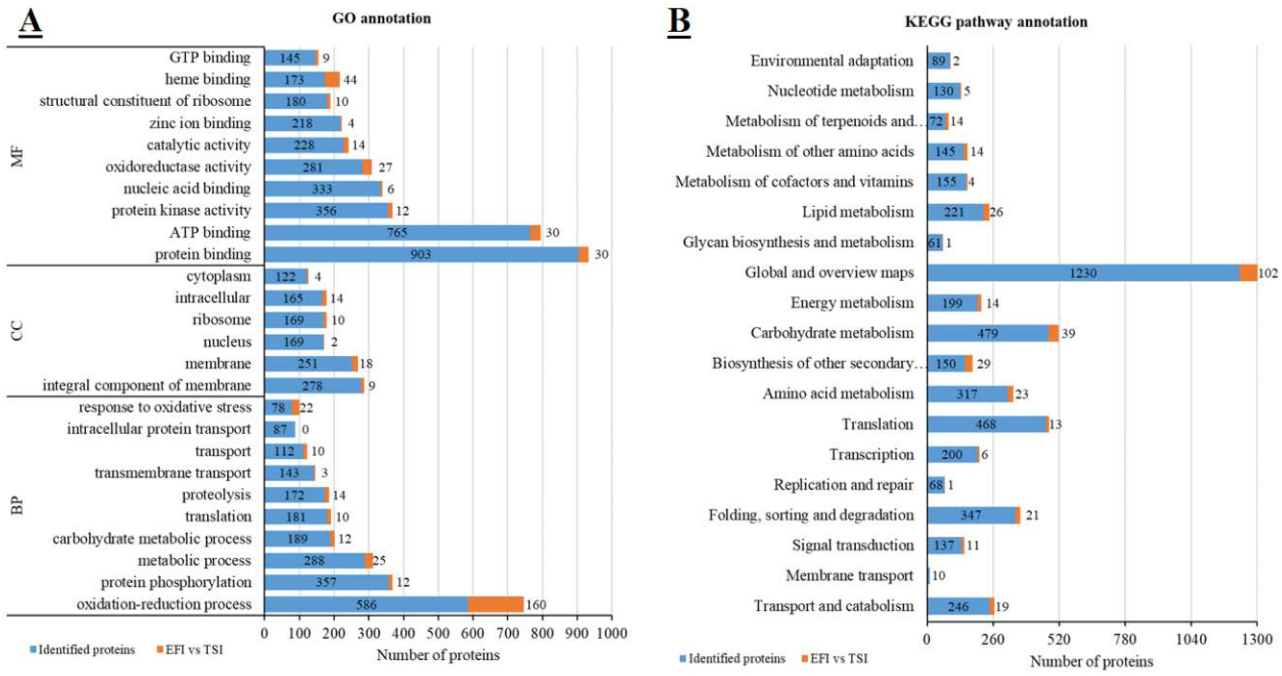

Figure 4. The GO (**A**) and KEGG (**B**) annotation of all identified proteins and DAPs (EFI vs. TSI). All proteins were classified by GO terms based on three categories: molecular function (MF), cellular component (CC), and biological process (BP).

According to KEGG annotation, 4724 identified proteins were grouped into 5 KO categories (i.e., cellular processes, environmental information processing, genetic information processing, metabolism, and organismal systems) (Figure 4B, Table S2). A total of 246 identified proteins (including 16 DAPs) were involved in cellular processes, 147 proteins (11 DAPs) were involved in environmental information processing, 1083 pro-

teins (41 DAPs) were involved in genetic information processing, 3159 proteins (271 DAPs) were involved in metabolism, and 89 proteins (2 DAPs) were involved in organismal systems.

According to the COG database, 5258 identified proteins were categorized into 25 categories (Figure 5A). The largest group was of general function prediction only (608); followed by translation, ribosomal structure, and biogenesis (559); post-translational modification, protein turnover, and chaperones (522); signal transduction mechanisms (476); carbohydrate transport and metabolism (456); amino acid transport and metabolism (308); lipid transport and metabolism (306); secondary metabolites' biosynthesis, transport, and catabolism (270); and energy production and conversion, followed by post-translation (255).

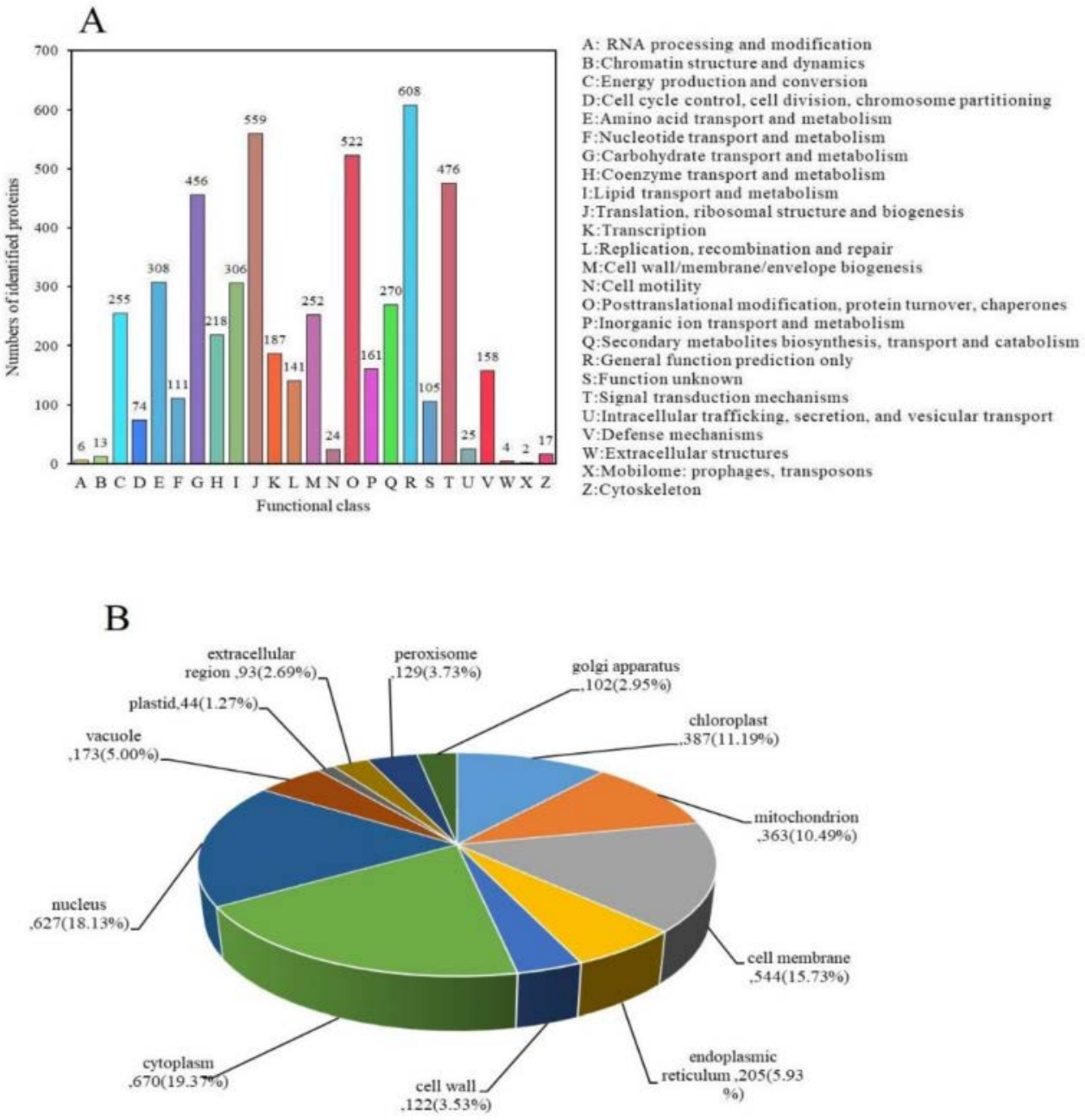

Figure 5. Categorization of all identified proteins with respect to COG annotation (**A**) and subcellular localization (**B**).

The subcellular location prediction and classification statistics for all identified proteins are shown in Figure 5B, and all identified proteins were classified into 12 subcellular

components according to their subcellular localizations, including 670 proteins in the cytoplasm (19.36%), 627 in the nucleus (18.12%), 544 in the cell membrane (15.73%), 387 in the chloroplast (11.19%), and 363 in the mitochondrion (10.49%).

3.3. Enrichment Analysis of DAPs

The expression profiles of the DAPs in six samples are presented through a heat map (Figure 6A). A total of 513 DAPs were identified with a fold-changes (FC) > 1.5 or <0.67 and $p \leq 0.05$ (Table S1). Among the DAPs, 283 were up-regulated, and 280 were down-regulated (Figure 6B).

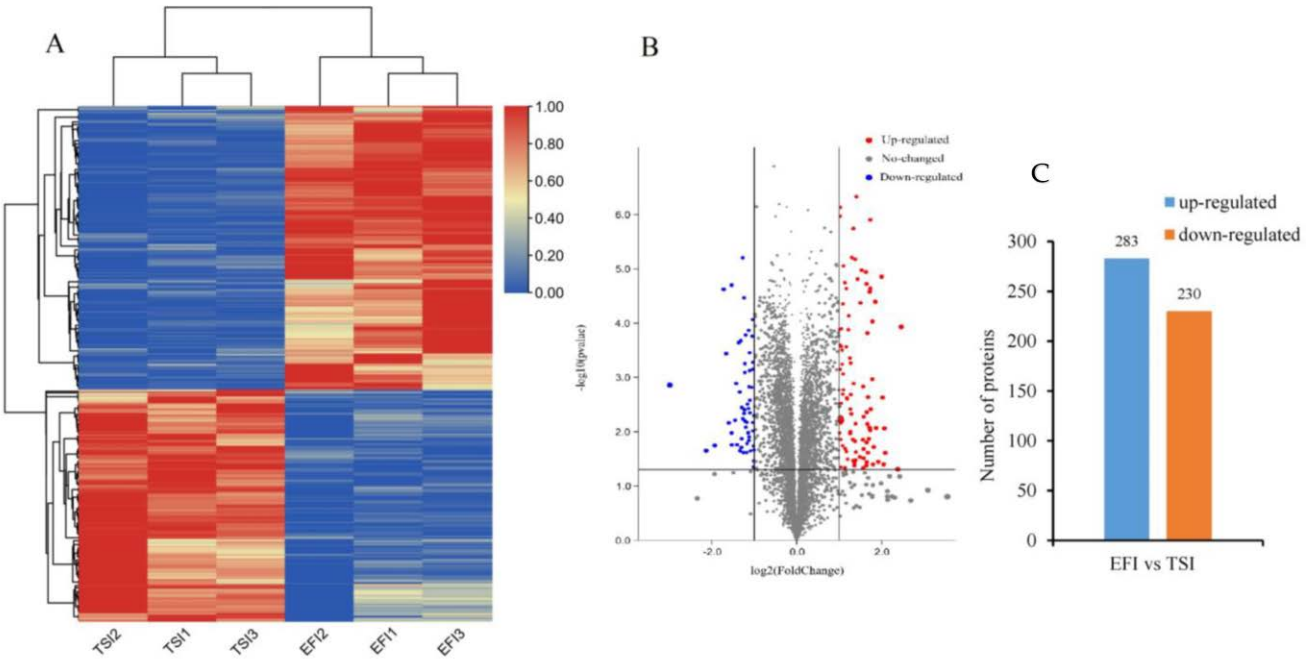

Figure 6. Effect of ebb-and-flow subirrigation strategy on proteome expressions of DAPs in tomato roots. (**A**) Expression profiles of the DAPs response to ebb-and-flow subirrigation. (**B**) Volcano plot of DAPs. (**C**) The numbers of up- and down-regulated proteins in the EFI treated plants compared to the TSI.

We completed an enrichment study of DAPs utilizing GO enrichment, KEGG pathways, and subcellular localization to see whether they were highly enriched in particular functional categories. The GO term meeting this requirement was determined as the GO term highly enriched in different proteins, using $p \leq 0.05$ as the threshold. With 222 GO terms, the 355 DAPs were divided into 3 groups: biological process (BP), cellular component (CC), and molecular function (MF). GO enrichment analysis showed that the metabolic process, single-organism process, and single-organism metabolic process were the most dominant BP terms with 195, 145, and 118 DAPs, respectively. Similarly, microtubule and the anchored component of the membrane were the major CC terms with 3 and 2 DAPs, respectively, while ion binding, oxidoreductase activity, and metal ion binding were the dominant MF terms with 58, 57, and 55 DAPs, respectively (Figure 7A).

The 180 DAPs were divided into different KEGG pathways, with 13 of them being enriched ($p \leq 0.05$). KEGG pathway enrichment revealed that 93, 71, 23, and 19 DAPs were linked to metabolic pathways, secondary metabolite production, phenylpropanoid biosynthesis, and protein processing in the endoplasmic reticulum, respectively (Figure 7B).

The 272 DAPs were classified into 12 subcellular components according to their subcellular localizations, including 56 proteins in the cytoplasm (20.59%), 49 in the cell membrane (18.01%), 25 in the cell wall (9.19%), 21 in the vacuole (7.72%), and 26 in the endoplasmic reticulum (9.56%) (Figure 7C).

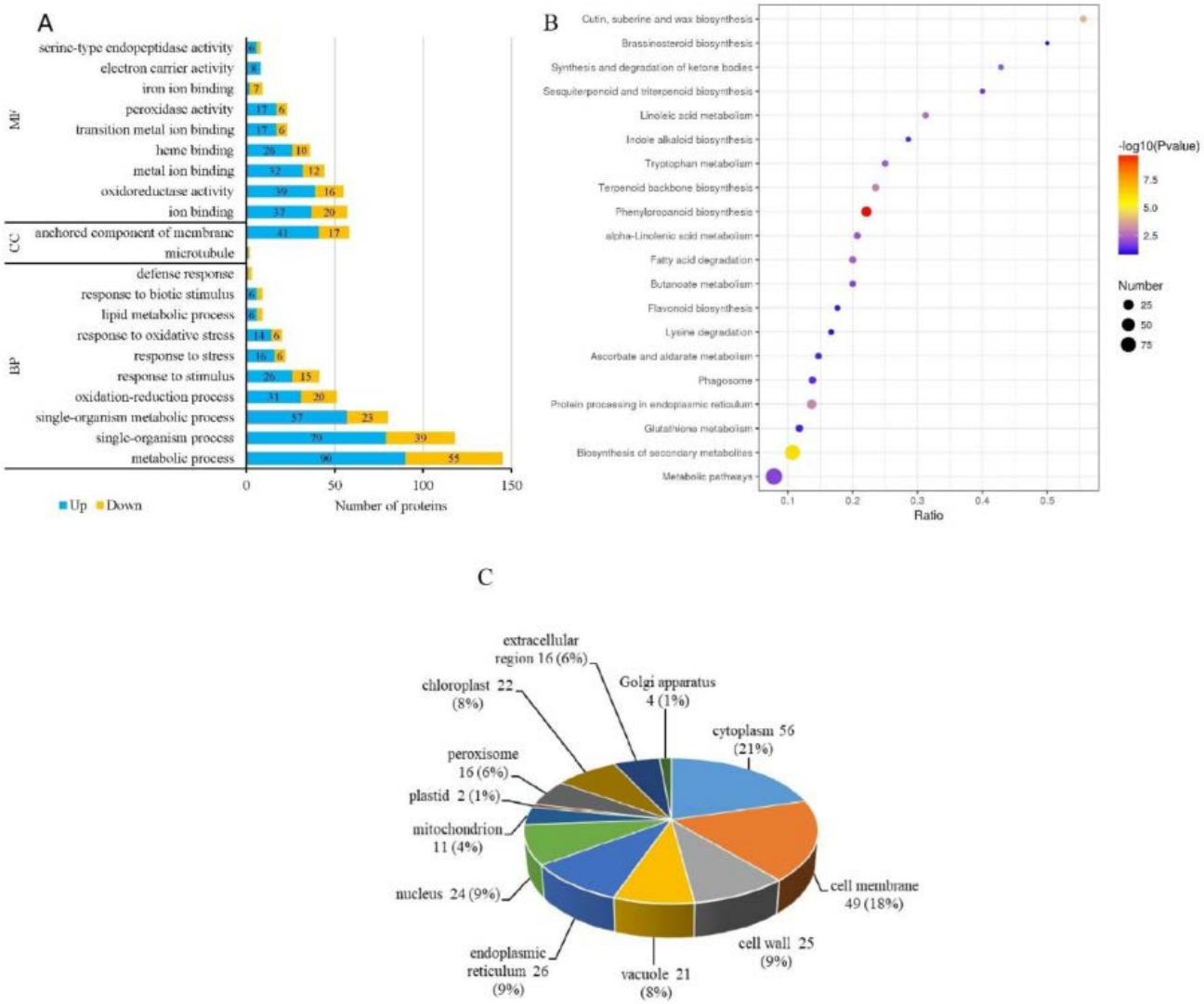

Figure 7. GO enrichment analysis (**A**) and KEGG enrichment analysis (**B**) and subcellular localizations (**C**) of DAPs in tomato roots under ebb-and-flow subirrigation.

3.4. Activities of Antioxidant Enzymes in Tomato Roots under Ebb-and-Flow Subirrigation

The activities of SOD, POD, CAT, APX, and GR in tomato roots under ebb-and-flow irrigation were significantly higher than those under top sprinkler irrigation, increasing by 12.99%, 16.98%, 18.25%, 46.51%, and 28.18%, respectively, while the content of MDA decreased significantly by 6.39% (Figure 8).

3.5. Correlation between Antioxidant Enzymes' Activities and Their Metabolism-Related Proteins

The correlation between antioxidant enzymes' activities (i.e., SOD, POD, CAT, GR, APX) and MDA content and their metabolism-related proteins in the roots of tomato seedlings grown under ebb-and-flow irrigation and top sprinkle irrigation was analyzed (Figure 9). The SOD and CAT activity was significantly ($p \leq 0.05$) and positively correlated with 11 SlPOD (Solyc10g076240.2.1, Solyc04g071900.3.1, Solyc01g105070.3.1, Solyc09g072700.3.1, Solyc09g007520.3.1, Solyc01g006300.3.1, Solyc11g018805.1.1, Solyc05g050870.3.1, Solyc01g015080.3.1, Solyc01g101050.3.1, and Solyc05g050890.2.1), 1 SlCAT Solyc12g094620.2.1, and 2 glutathione S-transferase proteins (Solyc09g011550.3.1 and Solyc08g066850.3.1). The POD activity was significantly ($p \leq 0.05$) and positively associated with 7 proteins related to peroxidase biosynthesis (Solyc10g076240.2.1, Solyc02g092580.3.1, Solyc01g105070.3.1,

Solyc05g046010.3.1, Solyc11g018805.1.1, Solyc01g101050.3.1, and Solyc05g050890.2.1), while 1 protein related to glutathione S-transferase synthesis (Solyc09g011550.3.1).

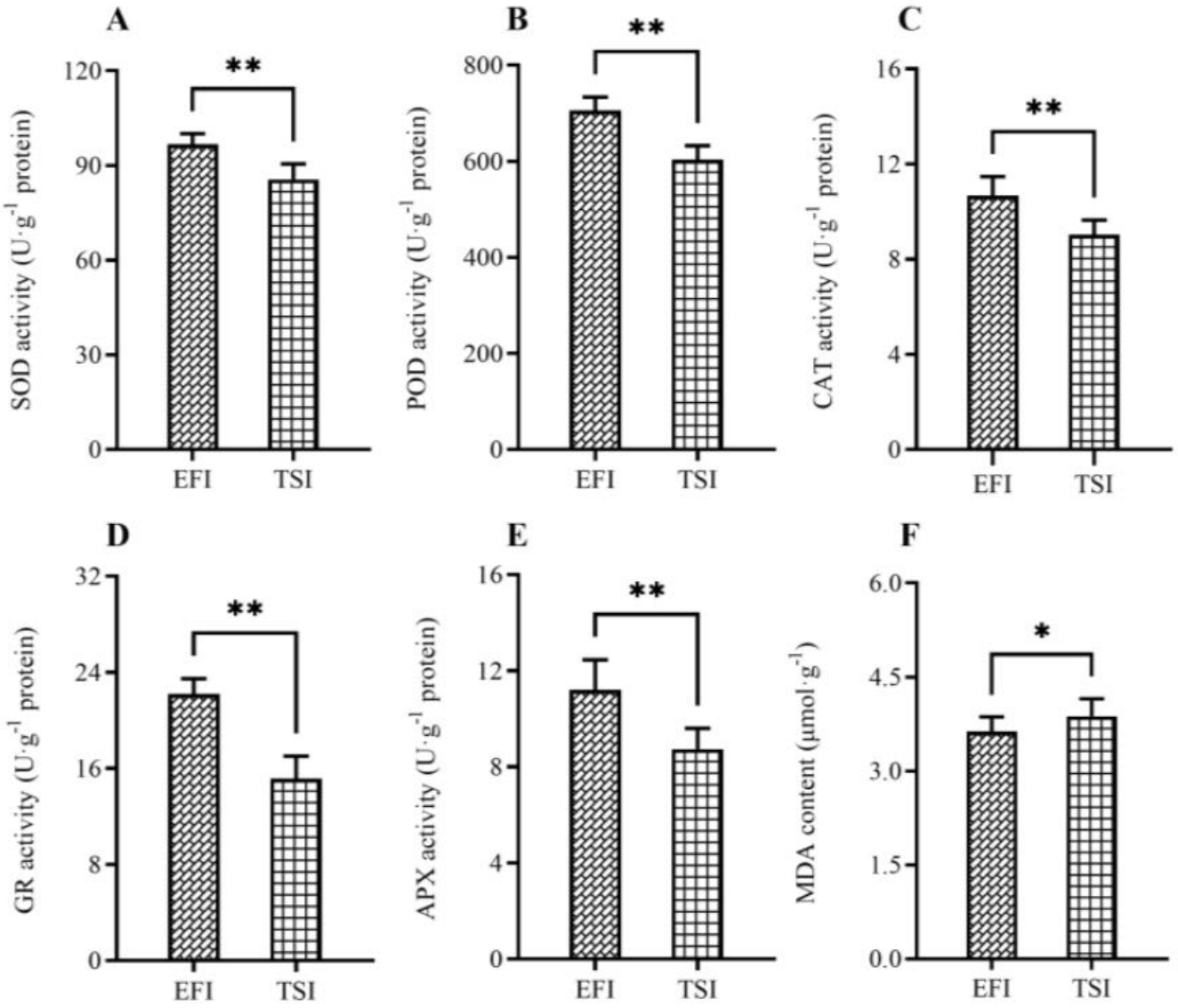

Figure 8. Effect of ebb-and-flow (EFI) irrigation and top sprinkle irrigation (TSI) on the activities of SOD (**A**), POD (**B**), CAT (**C**), GR (**D**), APX (**E**), and MDA content (**F**) of tomato roots. * and ** represent significance at $p \leq 0.05$ and $p \leq 0.01$, respectively.

Similarly, the GR activity was also significantly ($p \leq 0.05$) correlated with 13 proteins related to peroxidase and glutathione S-transferase biosynthesis (i.e., Solyc10g076240.2.1, Solyc04g071900.3.1, Solyc01g105070.3.1, Solyc05g046010.3.1, Solyc09g072700.3.1, Solyc09g007520.3.1, Solyc01g006300.3.1, Solyc11g018805.1.1, Solyc05g050870.3.1, Solyc01g101050.3.1, Solyc05g050890.2.1, Solyc09g011550.3.1, and Solyc08g066850.3.1). Thus, the activities of antioxidant enzymes were positively correlated with the expressions of their metabolism-related proteins.

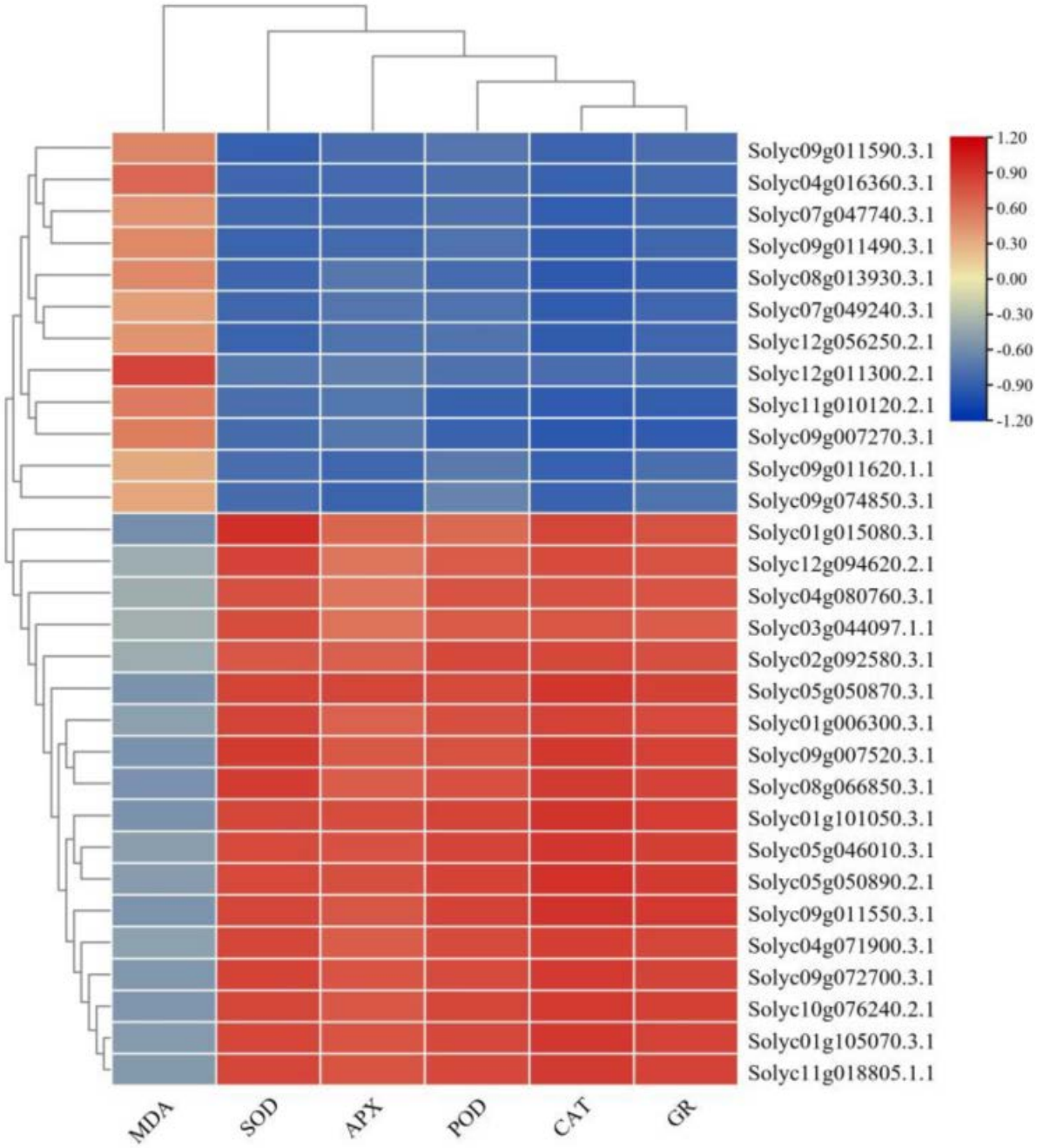

Figure 9. The heat map showing Pearson (*n*) correlation between antioxidant enzymes' activities and their metabolism-related proteins. Color codes: red—higher correlation; blue—lower correlation.

4. Discussion

In order to deeply understand the mechanism of ebb-and-flow subirrigation behind promoting seedling growth, the proteomic changes of tomato roots under two irrigation treatments were studied through the TMT-based quantitative proteomics method. A total of 513 DAPs were identified, of which 283 were up-regulated and 230 were down-regulated (Figure 7).

4.1. DAPs Participated in Carbohydrates and Energy Metabolism

Carbohydrates are essential for plants to maintain their life activities and are the main energy source for plants under abiotic stress [55]. In this experiment, it was found that ebb-and-flow irrigation treatment changed the proteomic expressions of 27 DAPs

related to energy metabolism. These DAPs were enriched into six major carbohydrate metabolism-related KEGG pathways (Table S3), namely, amino sugar and nucleotide sugar metabolism (ko00520), pyruvate metabolism (ko00620), glycolysis/gluconeogenesis (ko00010), galactose metabolism (ko00052), starch and sucrose metabolism (ko00500), and pentose and glucuronate interconversions (ko00040). There were eight DAPs involved in the glycolysis/gluconeogenesis pathway, of which six were up-regulated under EFI treatment, including aldehyde dehydrogenase (NAD+), alcohol dehydrogenase class-p, pyruvate decarboxylase, and L-lactate dehydrogenase. The results showed that ebb-and-flow irrigation increased the expression of carbohydrate-metabolism-related proteins in tomato roots, enhanced carbohydrate metabolism, promoted energy production in root cells, and ultimately promoted root growth [56,57]. Studies have shown that SS (sucrose synthase) in different plants was not only involved in sucrose accumulation [58,59] but also closely related to the growth status of plants under biological and abiotic stress [60]. Moreover, enzymes related to starch or sucrose metabolism accumulate more under drought conditions [61]. In this experiment, the proteins related to sucrose synthase and beta glucosidase were up-regulated under ebb-and-flow subirrigation.

4.2. DAPs Participated in Stress Resistance and Defense Response

A large number of reactive oxygen species (ROS) are produced in the plant body due to various stress conditions [62]. Plants have evolved to form a series of complex defense systems to deal with the impact of the adverse environment so as to protect cells from excessive ROS. Under ebb-and-flow irrigation, 30 DAPs related to stress and defense changed, including 17 up-regulated and 13 down-regulated DAPs (Table S4). These DAPs are mainly enriched in KEGG pathways, including phenylpropane biosynthesis (ko00940), ascorbic acid and aldarate metabolism (ko00053), glutathione metabolism (ko00480), and peroxisome (ko04146). The accumulation of POD and GST (glutathione S-transferase) in tomato roots was also increased (Figure 9), indicating that the increase in enzymatic activity of the antioxidant system under ebb-and-flow subirrigation was an important protective method of removing or reducing ROS accumulation. Relevant studies showed that under drought stress, the accumulation of GST in alfalfa 'Longzhong' roots also increased, protecting cells from oxidative stress [63].

Previous studies showed that the proteomic expression of CAT- and POD-metabolism-related proteins changed significantly under drought, high temperatures, and other stresses [64]. In this experiment, it was found that multiple DAPs encoding CAT and POD (i.e., Solyc12g094620.2.1, Solyc04g071900.3.1, Solyc01g105070.3.1, Solyc05g046010.3.1, Solyc03g044097.1.1, Solyc09g072700.3.1, Solyc09g007520.3.1, Solyc01g006300.3.1, and Solyc11g018805.1.1) were up-regulated, which was consistent with the higher activity of CAT and POD in tomato roots under ebb-and-flow irrigation (Figure 9). The DAPs related to the APX were also up-regulated. APX reduces the accumulation of hydrogen peroxide in plants through the ascorbic acid metabolic pathway [65]. Studies have shown that the levels of related proteins encoding APX change under heat stress, light stress, and water stress [66]. In this study, DAPs encoding APX and its analogs (Solyc11g062440.2.1, Solyc09g007270.3.1) were up-regulated so as to improve their activity in active oxygen metabolism. Under drought stress, the expression of proteins involved in phenylpropane metabolism also changes, such as cinnamyl alcohol dehydrogenase (CAD), peroxidase, and s-adenosine-l-methionine involved in lignin synthesis [67]. In this experiment, DAPs involved in phenylpropanoid biosynthesis (Solyc05g050870.3.1, Solyc01g015080.3.1, Solyc04g080760.3.1) and glutathione metabolism (Solyc09g01150.3.1, Solyc09g011620.1.1, Solyc12g011300.2.1, and Solyc09g074850.3.1) were also up-regulated. In general, stress-related proteins can eliminate ROS in time by promoting the activity of the antioxidant system so as to maintain the high vitality of tomato seedlings.

4.3. DAPs Participated in Amino Acid Metabolism

Amino acids are important proteins for plant growth, development, and response to various stresses [68,69]. Studies have shown that the abundance and expression of proline-, aspartate-, tryptophan-, and lysine-related proteins are severely influenced under drought or heat stress [70]. In the current study, 22 DAPs participated in the metabolic pathway of a variety of amino acids (Table S5), including tryptophan metabolism (ko00380); valine, leucine, and isoleucine degradation (ko00280); lysine degradation (ko00310); arginine and proline metabolism (ko00330); histidine metabolism (ko00340); beta-alanine metabolism (ko00410); tyrosine metabolism (ko00350); cysteine and methionine metabolism (ko00270); alanine, aspartate, and glutamate metabolism (ko00250); glycine, serine, and threonine metabolism (ko00260); and the biosynthesis of amino acids (ko01230). Aldehyde dehydrogenase (NAD +) was the main enzyme involved in lysine catabolism. The expressions of aldehyde-dehydrogenase-metabolism-related proteins were down-regulated in tomato roots under ebb-and-flow subirrigation. Similarly, asparagine synthase (glutamine-hydrolysing) was the main enzyme involved in asparagine synthesis, which was up-regulated in TSI, indicating that drought caused by TSI promotes the formation of asparagine from aspartic acid and glutamine to adapt to the drought stress. The up-regulated expression of threonine dehydratase and hydroxy-methyl-glutaryl-COA synthase in EFI may increase the biosynthesis of valine, leucine, and isoleucine, which can promote tomato root system development and secondary metabolism.

4.4. DAPs Participated in Plant Hormones and Secondary Metabolism

Plant hormones widely participate in the physiological process of plant growth and development [71] and play an important role in plant response to various environmental and biological stresses [72]. Studies have shown that GH3 family proteins influence the activity of amide synthase, which catalyzes the combination of free indoleacetic acid (IAA) and amino acids so as to inactivate it [73]. The IAA is released through the hydrolysis of IAA amide hydrolase to maintain the homeostasis of IAA in cells [74,75]. Abscisic acid (ABA) plays an important role in regulating seed germination [76], plant growth [77], and the response to stress [78]. In the present study, 79 DAPs were enriched in a large number of secondary-metabolism-related pathways, mainly including phenylpropanoid biosynthesis (ko00940); the biosynthesis of secondary metabolites (ko01110); cutin, suberine, and wax biosynthesis (ko00073); terpene main chain biosynthesis (ko00900), etc. (Table S6). It was identified that the auxin-responsive GH3 gene family showed down-regulated expression in EFI compared with TSI. Moreover, the synthesis of IAA was not inhibited, which promoted the normal growth of tomato roots. Additionally, it was identified that the related proteins of the ABA receptor PYR/PTL family showed down-regulated expressions under EFI, indicating that the synthesis of ABA was inhibited under the ebb-and-flow treatment so that the normal growth of tomato roots could not be inhibited.

5. Conclusions

In the present study, a TMT-based proteomic method was used to investigate changes in protein levels in roots of tomato seedlings grown under ebb-and-flow subirrigation and top sprinkle irrigation. In total, 8510 proteins and 513 DAPs were identified in tomato roots. The bioinformatic analysis revealed that these DAPs were involved in energy production and conversion, metabolic processes, the anchoring component of microtubule and membrane, oxidoreductase activity, and response to stimuli. The KEGG enrichment showed that the DAPs were enriched in 51 KEGG pathways, of which phenylpropane biosynthesis and secondary metabolite biosynthesis were the most significant pathways. The important pathways containing DAPs related to stress response were further divided into five categories, i.e., carbohydrate and energy metabolism, stress resistance and defense response, amino acid metabolism, plant hormones, and secondary metabolism. Ebb-and-flow subirrigation could significantly activate the expressions of proteins related to stress defense and ROS detoxification in tomato roots, which could effectively maintain the

balance of protein processing and degradation and enhance the ability of ion, electron, and protein transport across membranes and cell wall regulation so as to promote root growth.

Supplementary Materials: The following supporting information can be downloaded at: https://www.mdpi.com/article/10.3390/agronomy12081880/s1, Table S1: The detailed information about DAPs; Table S2: The KEGG annotation of identified proteins; Table S3: DAPs participated in carbohydrates and energy metabolism; Table S4: DAPs participated in stress resistance and defense response; Table S5: DAPs participated in amino acid metabolism; Table S6: DAPs participated in plant hormones and secondary metabolism.

Author Contributions: Conceptualization, K.W. and J.X.; methodology, K.W., T.G. and S.S.; software, K.W. and M.M.A.; validation, M.M.A., T.G. and F.C.; formal analysis, K.W. and M.M.A.; investigation, S.S. and X.C.; resources, J.X. and X.C.; data curation, M.M.A.; writing—original draft preparation, K.W. and M.M.A.; writing—review and editing, T.G., X.C., S.S., J.X. and F.C.; supervision, J.X. and F.C.; project administration, J.X. and K.W.; funding acquisition, J.X. and K.W. All authors have read and agreed to the published version of the manuscript.

Funding: This research was funded by 'China Agriculture Research System, grant number CARS-23' and the 'Doctoral Research Start Project of Wenzhou Vocational College of Science and Technology, grant number 201903'. 'Teacher professional development project of domestic visiting scholars in colleges and universities in 2021, grant number FX2021211'.

Institutional Review Board Statement: Not applicable.

Informed Consent Statement: Not applicable.

Data Availability Statement: The mass spectrometry proteomics data were deposited into the ProteomeXchange Consortium (http://proteomecentral.proteomexchange.org (accessed on 4 April 2022)) via the iProX partner repository [79] with the dataset identifier PXD033438.

Conflicts of Interest: The authors declare no conflict of interest.

References

1. Bai, Y.; Lindhout, P. Domestication and Breeding of Tomatoes: What have We Gained and What Can We Gain in the Future? *Ann. Bot.* **2007**, *100*, 1085–1094. [CrossRef] [PubMed]
2. Yousef, A.F.; Ali, M.M.; Rizwan, H.M.; Gad, A.G.; Liang, D.; Binqi, L.; Kalaji, H.M.; Wróbel, J.; Xu, Y.; Chen, F. Light quality and quantity affect graft union formation of tomato plants. *Sci. Rep.* **2021**, *11*, 9870. [CrossRef] [PubMed]
3. Guo, T.; Gull, S.; Ali, M.M.; Yousef, A.F.; Ercisli, S.; Kalaji, H.M.; Telesiński, A.; Auriga, A.; Wróbel, J.; Radwan, N.S.; et al. Heat stress mitigation in tomato (*Solanum lycopersicum* L.) through foliar application of gibberellic acid. *Sci. Rep.* **2022**, *12*, 11324. [CrossRef] [PubMed]
4. Al-Muhtaseb, A.H.; Al-Harahsheh, M.; Hararah, M.; Magee, T.R.A. Drying characteristics and quality change of unutilized-protein rich-tomato pomace with and without osmotic pre-treatment. *Ind. Crops Prod.* **2010**, *31*, 171–177. [CrossRef]
5. Ali, M.M.; Waleed Shafique, M.; Gull, S.; Afzal Naveed, W.; Javed, T.; Yousef, A.F.; Mauro, R.P. Alleviation of Heat Stress in Tomato by Exogenous Application of Sulfur. *Horticulturae* **2021**, *7*, 21. [CrossRef]
6. Yousef, A.F.; Xu, Y.; Chen, F.; Lin, K.; Zhang, X.; Guiamba, H.; Ibrahim, M.M.; Rizwan, H.M.; Ali, M.M. The influence of LEDs light quality on the growth pigments biochemical and chlorophyll fluorescence characteristics of tomato seedlings (*Solanum lycopersicum* L.). *Fresenius Environ. Bull.* **2021**, *30*, 3575–3588.
7. Yousef, A.F.; Ali, M.M.; Rizwan, H.M.; Tadda, S.A.; Xu, Y.; Kalaji, H.M.; Yang, H.; Ahmed, M.A.A.; Wro, J.; Chen, F. Photosynthetic apparatus performance of tomato seedlings grown under various combinations of LED illumination. *PLoS ONE* **2021**, *16*, e0249373. [CrossRef]
8. Ali, M.M.; Javed, T.; Mauro, R.P.; Shabbir, R.; Afzal, I.; Yousef, A.F. Effect of Seed Priming with Potassium Nitrate on the Performance of Tomato. *Agriculture* **2020**, *10*, 498. [CrossRef]
9. Richards, D.L.; Reed, D.W. New Guinea Impatiens Growth Response and Nutrient Release from Controlled-release Fertilizer in a Recirculating Subirrigation and Top-watering System. *HortScience* **2004**, *39*, 280–286. [CrossRef]
10. Zheng, Y.; Graham, T.; Richard, S.; Dixon, M. Potted Gerbera Production in a Subirrigation System Using Low-concentration Nutrient Solutions. *HortScience* **2004**, *39*, 1283–1286. [CrossRef]
11. Zheng, Y.; Graham, T.; Richard, S.; Dixon, M. Can Low Nutrient Strategies be used for Pot Gerbera Production in Closed-Loop Subirrigation? *Acta Hortic.* **2005**, *691*, 365–372. [CrossRef]
12. Ferrarezi, R.S.; Weaver, G.M.; van Iersel, M.W.; Testezlaf, R. Subirrigation: Historical Overview, Challenges, and Future Prospects. *Horttechnology* **2015**, *25*, 262–276. [CrossRef]

13. Araus, J.L.; Rezzouk, F.Z.; Thushar, S.; Shahid, M.; Elouafi, I.A.; Bort, J.; Serret, M.D. Effect of irrigation salinity and ecotype on the growth, physiological indicators and seed yield and quality of Salicornia europaea. *Plant Sci.* **2021**, *304*, 110819. [CrossRef]
14. Fereres, E.; Soriano, M.A. Deficit irrigation for reducing agricultural water use. *J. Exp. Bot.* **2006**, *58*, 147–159. [CrossRef]
15. Morison, J.I.; Baker, N.; Mullineaux, P.; Davies, W. Improving water use in crop production. *Philos. Trans. R. Soc. B Biol. Sci.* **2008**, *363*, 639–658. [CrossRef]
16. Nadeem, M.; Li, J.; Yahya, M.; Sher, A.; Ma, C.; Wang, X.; Qiu, L. Research Progress and Perspective on Drought Stress in Legumes: A Review. *Int. J. Mol. Sci.* **2019**, *20*, 2541. [CrossRef]
17. Parkash, V.; Singh, S.; Deb, S.K.; Ritchie, G.L.; Wallace, R.W. Effect of deficit irrigation on physiology, plant growth, and fruit yield of cucumber cultivars. *Plant Stress* **2021**, *1*, 100004. [CrossRef]
18. Leskovar, D.I. Root and Shoot Modification by Irrigation. *Horttechnology* **1998**, *8*, 510–514. [CrossRef]
19. Elmer, W.H.; Gent, M.P.N.; McAvoy, R.J. Partial saturation under ebb and flow irrigation suppresses Pythium root rot of ornamentals. *Crop Prot.* **2012**, *33*, 29–33. [CrossRef]
20. James, E.; van Iersel, M. Ebb and Flow Production of Petunias and Begonias as Affected by Fertilizers with Different Phosphorus Content. *HortScience* **2001**, *36*, 282–285. [CrossRef]
21. Buwalda, F.; Baas, R.; van Weel, P.A. A soilless ebb-and-flow system for all-year-round chrysanthemums. *Acta Hortic.* **1994**, *361*, 123–132. [CrossRef]
22. Naghedifar, S.M.; Ziaei, A.N.; Ansari, H. Numerical analysis of sensor-based flood-floor ebb-and-flow subirrigation system with saline water. *Arch. Agron. Soil Sci.* **2021**, *67*, 1285–1299. [CrossRef]
23. Poole, R.T.; Conover, C.A. Fertilizer Levels and Medium Affect Foliage Plant Growth in an Ebb and Flow Irrigation System. *J. Environ. Hortic.* **1992**, *10*, 81–86. [CrossRef]
24. Rouphael, Y.; Cardarelli, M.; Rea, E.; Colla, G. The influence of irrigation system and nutrient solution concentration on potted geranium production under various conditions of radiation and temperature. *Sci. Hortic.* **2008**, *118*, 328–337. [CrossRef]
25. Leskovar, D.I.; Boales, A.K. Plant Establishment Systems Affect Yield of Jalapeno Pepper. *Acta Hortic.* **1995**, *412*, 275–280. [CrossRef]
26. Leskovar, D.I.; Cantliffe, D.J. Comparison of Plant Establishment Method, Transplant, or Direct Seeding on Growth and Yield of Bell Pepper. *J. Am. Soc. Hortic. Sci.* **1993**, *118*, 17–22. [CrossRef]
27. Leskovar, D.I.; Cantliffe, D.J.; Stoffella, P.J. Transplant Production Systems Influence Growth and Yield of Fresh-market Tomatoes. *J. Am. Soc. Hortic. Sci.* **1994**, *119*, 662–668. [CrossRef]
28. Mahgoub, N.A.; Ibrahim, A.M.; Ali, O.M. Effect of different irrigation systems on root growth of maize and cowpea plants in sandy soil. *Eur. J. Soil Sci.* **2017**, *6*, 374–379. [CrossRef]
29. Xuewen, X.; Huihui, W.; Xiaohua, Q.; Qiang, X.; Xuehao, C. Waterlogging-induced increase in fermentation and related gene expression in the root of cucumber (*Cucumis sativus* L.). *Sci. Hortic.* **2014**, *179*, 388–395. [CrossRef]
30. Zhang, P.; Lyu, D.; Jia, L.; He, J.; Qin, S. Physiological and de novo transcriptome analysis of the fermentation mechanism of *Cerasus sachalinensis* roots in response to short-term waterlogging. *BMC Genom.* **2017**, *18*, 649. [CrossRef]
31. Hattori, Y.; Nagai, K.; Furukawa, S.; Song, X.-J.; Kawano, R.; Sakakibara, H.; Wu, J.; Matsumoto, T.; Yoshimura, A.; Kitano, H.; et al. The ethylene response factors SNORKEL1 and SNORKEL2 allow rice to adapt to deep water. *Nature* **2009**, *460*, 1026–1030. [CrossRef] [PubMed]
32. Kuroha, T.; Nagai, K.; Gamuyao, R.; Wang, D.R.; Furuta, T.; Nakamori, M.; Kitaoka, T.; Adachi, K.; Minami, A.; Mori, Y.; et al. Ethylene-gibberellin signaling underlies adaptation of rice to periodic flooding. *Science* **2018**, *361*, 181–186. [CrossRef] [PubMed]
33. Pan, J.; Sharif, R.; Xu, X.; Chen, X. Mechanisms of Waterlogging Tolerance in Plants: Research Progress and Prospects. *Front. Plant Sci.* **2021**, *11*, 627331. [CrossRef] [PubMed]
34. Fukao, T.; Barrera-Figueroa, B.E.; Juntawong, P.; Peña-Castro, J.M. Submergence and Waterlogging Stress in Plants: A Review Highlighting Research Opportunities and Understudied Aspects. *Front. Plant Sci.* **2019**, *10*, 340. [CrossRef] [PubMed]
35. Anee, T.I.; Nahar, K.; Rahman, A.; Mahmud, J.A.; Bhuiyan, T.F.; Alam, M.U.; Fujita, M.; Hasanuzzaman, M. Hasanuzzaman Oxidative Damage and Antioxidant Defense in Sesamum indicum after Different Waterlogging Durations. *Plants* **2019**, *8*, 196. [CrossRef]
36. Habibullah, M.; Sarkar, S.; Islam, M.M.; Ahmed, K.U.; Rahman, M.Z.; Awad, M.F.; ElSayed, A.I.; Mansour, E.; Hossain, M.S. Assessing the Response of Diverse Sesame Genotypes to Waterlogging Durations at Different Plant Growth Stages. *Plants* **2021**, *10*, 2294. [CrossRef]
37. Liu, Y.; Cao, D.; Ma, L.; Jin, X.; Yang, P.; Ye, F.; Liu, P.; Gong, Z.; Wei, C. TMT-based quantitative proteomics analysis reveals the response of tea plant (*Camellia sinensis*) to fluoride. *J. Proteom.* **2018**, *176*, 71–81. [CrossRef]
38. Hao, J.; Guo, H.; Shi, X.; Wang, Y.; Wan, Q.; Song, Y.-B.; Zhang, L.; Dong, M.; Shen, C. Comparative proteomic analyses of two Taxus species (Taxus× media and Taxus mairei) reveals variations in the metabolisms associated with paclitaxel and other metabolites. *Plant Cell Physiol.* **2017**, *58*, 1878–1890. [CrossRef]
39. Xu, D.; Yuan, H.; Tong, Y.; Zhao, L.; Qiu, L.; Guo, W.; Shen, C.; Liu, H.; Yan, D.; Zheng, B. Comparative Proteomic Analysis of the Graft Unions in Hickory (*Carya cathayensis*) Provides Insights into Response Mechanisms to Grafting Process. *Front. Plant Sci.* **2017**, *8*, 676. [CrossRef]
40. Kelei, W.; Youhe, Z.; Jianlei, S.; Zong'an, H.; Longjing, Z.; Jian, X. Application of dynamic water level management of ebb and flow irrigation for cucumber seedlings. *Acta Agric. Zhejiangensis* **2017**, *29*, 408–413.

41. Chao, Y.-Y.; Chen, C.-Y.; Huang, W.-D.; Kao, C.H. Salicylic acid-mediated hydrogen peroxide accumulation and protection against Cd toxicity in rice leaves. *Plant Soil* **2010**, *329*, 327–337. [CrossRef]
42. El-Shabrawi, H.; Kumar, B.; Kaul, T.; Reddy, M.K.; Singla-Pareek, S.L.; Sopory, S.K. Redox homeostasis, antioxidant defense, and methylglyoxal detoxification as markers for salt tolerance in Pokkali rice. *Protoplasma* **2010**, *245*, 85–96. [CrossRef]
43. Hasanuzzaman, M.; Hossain, M.A.; Fujita, M. Nitric oxide modulates antioxidant defense and the methylglyoxal detoxification system and reduces salinity-induced damage of wheat seedlings. *Plant Biotechnol. Rep.* **2011**, *5*, 353–365. [CrossRef]
44. Zhou, Y.; Ming, D.; Cui, J.; Chen, X.; Wen, Z.; Zhang, J.; Liu, H. Exogenous GSH protects tomatoes against salt stress by modulating photosystem II efficiency, absorbed light allocation and H_2O_2-scavenging system in chloroplasts. *J. Integr. Agric.* **2018**, *17*, 2257–2272. [CrossRef]
45. Nakano, Y.; Asada, K. Hydrogen Peroxide is Scavenged by Ascorbate-specific Peroxidase in Spinach Chloroplasts. *Plant Cell Physiol.* **1981**, *22*, 867–880. [CrossRef]
46. Cakmak, I.; Strbac, D.; Marschner, H. Activities of Hydrogen Peroxide-Scavenging Enzymes in Germinating Wheat Seeds. *J. Exp. Bot.* **1993**, *44*, 127–132. [CrossRef]
47. Hao, P.; Zhu, J.; Gu, A.; Lv, D.; Ge, P.; Chen, G.; Li, X.; Yan, Y. An integrative proteome analysis of different seedling organs in tolerant and sensitive wheat cultivars under drought stress and recovery. *Proteomics* **2015**, *15*, 1544–1563. [CrossRef]
48. Chen, C.; Chen, H.; Zhang, Y.; Thomas, H.R.; Frank, M.H.; He, Y.; Xia, R. TBtools: An Integrative Toolkit Developed for Interactive Analyses of Big Biological Data. *Mol. Plant* **2020**, *13*, 1194–1202. [CrossRef]
49. Jones, P.; Binns, D.; Chang, H.-Y.; Fraser, M.; Li, W.; McAnulla, C.; McWilliam, H.; Maslen, J.; Mitchell, A.; Nuka, G.; et al. InterProScan 5: Genome-scale protein function classification. *Bioinformatics* **2014**, *30*, 1236–1240. [CrossRef]
50. Huang, D.W.; Sherman, B.T.; Lempicki, R.A. Bioinformatics enrichment tools: Paths toward the comprehensive functional analysis of large gene lists. *Nucleic Acids Res.* **2009**, *37*, 1–13. [CrossRef]
51. Horton, P.; Park, K.-J.; Obayashi, T.; Fujita, N.; Harada, H.; Adams-Collier, C.J.; Nakai, K. WoLF PSORT: Protein localization predictor. *Nucleic Acids Res.* **2007**, *35*, W585–W587. [CrossRef] [PubMed]
52. Goldberg, T.; Hecht, M.; Hamp, T.; Karl, T.; Yachdav, G.; Ahmed, N.; Altermann, U.; Angerer, P.; Ansorge, S.; Balasz, K.; et al. LocTree3 prediction of localization. *Nucleic Acids Res.* **2014**, *42*, W350–W355. [CrossRef] [PubMed]
53. Emanuelsson, O.; Nielsen, H.; Brunak, S.; von Heijne, G. Predicting Subcellular Localization of Proteins Based on their N-terminal Amino Acid Sequence. *J. Mol. Biol.* **2000**, *300*, 1005–1016. [CrossRef] [PubMed]
54. Petersen, T.N.; Brunak, S.; von Heijne, G.; Nielsen, H. SignalP 4.0: Discriminating signal peptides from transmembrane regions. *Nat. Methods* **2011**, *8*, 785–786. [CrossRef] [PubMed]
55. Ghosh, D.; Xu, J. Abiotic stress responses in plant roots: A proteomics perspective. *Front. Plant Sci.* **2014**, *5*, 6. [CrossRef]
56. Chen, T.; Zhang, L.; Shang, H.; Liu, S.; Peng, J.; Gong, W.; Shi, Y.; Zhang, S.; Li, J.; Gong, J.; et al. iTRAQ-Based Quantitative Proteomic Analysis of Cotton Roots and Leaves Reveals Pathways Associated with Salt Stress. *PLoS ONE* **2016**, *11*, e0148487. [CrossRef] [PubMed]
57. Yao, K.; Wu, Y.Y. Phosphofructokinase and glucose-6-phosphate dehydrogenase in response to drought and bicarbonate stress at transcriptional and functional levels in mulberry. *Russ. J. Plant Physiol.* **2016**, *63*, 235–242. [CrossRef]
58. Yu, X.; Ali, M.M.; Li, B.; Fang, T.; Chen, F. Transcriptome data-based identification of candidate genes involved in metabolism and accumulation of soluble sugars during fruit development in 'Huangguan' plum. *J. Food Biochem.* **2021**, *45*, e13878. [CrossRef]
59. Pan, T.; Ali, M.M.; Gong, J.; She, W.; Pan, D.; Guo, Z.; Yu, Y.; Chen, F. Fruit Physiology and Sugar-Acid Profile of 24 Pomelo (*Citrus grandis* (L.) Osbeck) Cultivars Grown in Subtropical Region of China. *Agronomy* **2021**, *11*, 2393. [CrossRef]
60. Park, J.-Y.; Canam, T.; Kang, K.-Y.; Ellis, D.D.; Mansfield, S.D. Over-expression of an arabidopsis family A sucrose phosphate synthase (SPS) gene alters plant growth and fibre development. *Transgenic Res.* **2008**, *17*, 181–192. [CrossRef]
61. Tian, H.; Ma, L.; Zhao, C.; Hao, H.; Gong, B.; Yu, X.; Wang, X. Antisense repression of sucrose phosphate synthase in transgenic muskmelon alters plant growth and fruit development. *Biochem. Biophys. Res. Commun.* **2010**, *393*, 365–370. [CrossRef]
62. Wang, K.; Ali, M.M.; Pan, K.; Su, S.; Xu, J.; Chen, F. Ebb-and-Flow Subirrigation Improves Seedling Growth and Root Morphology of Tomato by Influencing Root-Softening Enzymes and Transcript Profiling of Related Genes. *Agronomy* **2022**, *12*, 494. [CrossRef]
63. Zhang, C.; Shi, S. Physiological and Proteomic Responses of Contrasting Alfalfa (*Medicago sativa* L.) Varieties to PEG-Induced Osmotic Stress. *Front. Plant Sci.* **2018**, *9*, 242. [CrossRef]
64. Du, C.; Chai, L.; Wang, Z.; Fan, H. Response of proteome and morphological structure to short-term drought and subsequent recovery in Cucumis sativus leaves. *Physiol. Plant.* **2019**, *167*, 676–689. [CrossRef]
65. Mathews, M.C.; Summers, C.B.; Felton, G.W. Ascorbate peroxidase: A novel antioxidant enzyme in insects. *Arch. Insect Biochem. Physiol.* **1997**, *34*, 57–68. [CrossRef]
66. Choi, S.; Jeong, S.; Jeong, W.; Kwon, S.; Chow, W.; Park, Y.-I. Chloroplast Cu/Zn-superoxide dismutase is a highly sensitive site in cucumber leaves chilled in the light. *Planta* **2002**, *216*, 315–324. [CrossRef]
67. Tu, Y.; Rochfort, S.; Liu, Z.; Ran, Y.; Griffith, M.; Badenhorst, P.; Louie, G.V.; Bowman, M.E.; Smith, K.F.; Noel, J.P.; et al. Functional Analyses of Caffeic Acid O-Methyltransferase and Cinnamoyl-CoA-Reductase Genes from Perennial Ryegrass (*Lolium perenne*). *Plant Cell* **2010**, *22*, 3357–3373. [CrossRef]
68. Hu, W.; Wang, B.; Ali, M.M.; Chen, X.; Zhang, J.; Zheng, S.; Chen, F. Free Amino Acids Profile and Expression Analysis of Core Genes Involved in Branched-Chain Amino Acids Metabolism during Fruit Development of Longan (*Dimocarpus longan* Lour.) Cultivars with Different Aroma Types. *Biology* **2021**, *10*, 807. [CrossRef]

69. Zhi, C.; Ali, M.M.; Zhang, J.; Shi, M.; Ma, S.; Chen, F. Effect of Paper and Aluminum Bagging on Fruit Quality of Loquat (*Eriobotrya japonica* Lindl.). *Plants* **2021**, *10*, 2704. [CrossRef]
70. Cao, L.; Lu, X.; Zhang, P.; Wang, G.; Wei, L.; Wang, T. Systematic Analysis of Differentially Expressed Maize ZmbZIP Genes between Drought and Rewatering Transcriptome Reveals bZIP Family Members Involved in Abiotic Stress Responses. *Int. J. Mol. Sci.* **2019**, *20*, 4103. [CrossRef]
71. Ali, M.M.; Anwar, R.; Malik, A.U.; Khan, A.S.; Ahmad, S.; Hussain, Z.; Hasan, M.U.; Nasir, M.; Chen, F. Plant Growth and Fruit Quality Response of Strawberry is Improved After Exogenous Application of 24-Epibrassinolide. *J. Plant Growth Regul.* **2022**, *41*, 1786–1799. [CrossRef]
72. Ali, M.M.; Yousef, A.F.; Li, B.; Chen, F. Effect of Environmental Factors on Growth and Development of Fruits. *Trop. Plant Biol.* **2021**, *14*, 226–238. [CrossRef]
73. Staswick, P.E.; Serban, B.; Rowe, M.; Tiryaki, I.; Maldonado, M.T.; Maldonado, M.C.; Suza, W. Characterization of an Arabidopsis Enzyme Family That Conjugates Amino Acids to Indole-3-Acetic Acid. *Plant Cell* **2005**, *17*, 616–627. [CrossRef]
74. Chen, Y.; Shen, H.; Wang, M.; Li, Q.; He, Z. Salicyloyl-aspartate synthesized by the acetyl-amido synthetase GH3.5 is a potential activator of plant immunity in Arabidopsis. *Acta Biochim. Biophys. Sin.* **2013**, *45*, 827–836. [CrossRef]
75. Yang, Y.; Yue, R.; Sun, T.; Zhang, L.; Chen, W.; Zeng, H.; Wang, H.; Shen, C. Genome-wide identification, expression analysis of GH3 family genes in Medicago truncatula under stress-related hormones and Sinorhizobium meliloti infection. *Appl. Microbiol. Biotechnol.* **2015**, *99*, 841–854. [CrossRef]
76. Finkelstein, R.R.; Lynch, T.J. The Arabidopsis Abscisic Acid Response Gene ABI5 Encodes a Basic Leucine Zipper Transcription Factor. *Plant Cell* **2000**, *12*, 599–609. [CrossRef]
77. Zhao, W.; Guan, C.; Feng, J.; Liang, Y.; Zhan, N.; Zuo, J.; Ren, B. The Arabidopsis CROWDED NUCLEI genes regulate seed germination by modulating degradation of ABI5 protein. *J. Integr. Plant Biol.* **2016**, *58*, 669–678. [CrossRef]
78. Mittal, A.; Gampala, S.S.L.; Ritchie, G.L.; Payton, P.; Burke, J.J.; Rock, C.D. Related to ABA-Insensitive3(ABI3)/Viviparous1 and AtABI5 transcription factor coexpression in cotton enhances drought stress adaptation. *Plant Biotechnol. J.* **2014**, *12*, 578–589. [CrossRef]
79. Ma, J.; Chen, T.; Wu, S.; Yang, C.; Bai, M.; Shu, K.; Li, K.; Zhang, G.; Jin, Z.; He, F.; et al. iProX: An integrated proteome resource. *Nucleic Acids Res.* **2019**, *47*, D1211–D1217. [CrossRef]